

Original Article

A novel positive feedback regulation between long noncoding RNA UICC and IL-6/STAT3 signaling promotes cervical cancer progression

Ke Su, Qian Zhao, Aiping Bian, Chunfang Wang, Yujie Cai, Yanyan Zhang

Department of Gynecology, The First Affiliated Hospital of Zhengzhou University, Zhengzhou 450052, Henan Province, P. R. China

Received June 10, 2018; Accepted June 26, 2018; Epub July 1, 2018; Published July 15, 2018

Abstract: Long noncoding RNAs (lncRNAs), a novel class of transcripts that have critical roles in carcinogenesis and progression, have emerged as important gene expression modulators. However, the pathophysiological contributions and the underlying mechanisms of specific lncRNAs in cervical cancer remain largely unknown. Here, using transcriptome microarray analysis, we identified a novel lncRNA termed lncRNA upregulated in cervical cancer (lnc-UICC) that was highly expressed in cervical cancer tissue. lnc-UICC expression in cervical cancer was associated with FIGO stage, lymph node metastasis and prognosis. Through gain- and loss-of-lnc-UICC expression, we found lnc-UICC could significantly promote tumor growth and metastasis *in vitro* and *in vivo*. Mechanistically, lnc-UICC promoted STAT3 activation through two complementary ways. lnc-UICC could regulate the IL-6 transcription through binding to IL-6 promoter. lnc-UICC also directly interacted with the phospho-STAT3, and increased its protein stability by protecting it from proteasome-dependent degradation. Moreover, we revealed that lnc-UICC was a STAT3-responsive lncRNA, as STAT3 could bind to the lnc-UICC promoter to enhance its transcription, suggesting that there exists a positive feedback loop between lnc-UICC and IL-6/STAT3 signaling. In sum, therefore, we have identified an lncRNA-based IL-6/STAT3 signaling regulatory circuit that promotes tumorigenesis and metastasis in cervical cancer cells, highlighting the role that lncRNAs can play in tumor progression.

Keywords: lncRNA, cervical cancer, feedback loop, IL-6/STAT3

Introduction

As one of the most malignant cancers, cervical cancer accounts for a large proportion of cancer-associated mortalities among women worldwide. It has been reported that there are more than 530,000 new cases annually, and approximately 275,000 deaths due to cervical cancer per year [1]. Even though the patients suffering from cervical cancer can receive relevant treatments such as surgery, chemotherapy, radiotherapy and targeted therapy, the overall survival rates of them are still unsatisfactory [2]. Therefore, a deepgoing study on the molecular and functional mechanism of cervical cancer is urgently necessary.

Long noncoding RNAs (lncRNAs), more than 200 nucleotides in length, do not have any apparent protein-coding ability and are impor-

tant members of the noncoding RNA family. lncRNAs are evolutionarily conserved and act as crucial regulators in modulating cellular proliferation, migration, invasion and cancer stem cells' self-renewal [3, 4]. lncRNAs regulate gene expression through diverse mechanisms, such as chromatin modification, epigenetic regulation, DNA methylation, gene imprinting, and RNA splicing [5, 6]. Accumulating evidence has reported the relationship between lncRNAs and the initiation and progression of many cancers [4]. The aberrant expression of lncRNAs has been observed in multiple malignancies, including cervical cancer [7]. However, the pathophysiological contributions and the underlying molecular mechanisms of specific lncRNAs in cervical cancer remain largely unknown. In the current study, we report the identification of lncRNA upregulated in cervical cancer (lnc-UICC, GeneSymbol: BC038578), and elucidated

Inc-UICC promotes cervical cancer progression

its oncogenic role in cervical cancer progression via IL-6/STAT3 signaling.

Materials and methods

Cell culture

Caski, SiHa, HeLa, Ms751 and C33a cells were purchased from the American Type Culture Collection (ATCC; Manassas, VA, USA). Cells were cultured in DMEM/F-12 (Gibco, USA) with 10% FBS (Gibco, USA) at 37°C in a humidified 5% CO₂.

Clinical samples

A total of 68 cervical cancer tissues and adjacent non-tumor tissues were obtained from The First Affiliated Hospital of Zhengzhou University between 2012 and 2017. Samples were selected based on the diagnosis of cervical cancer, determined by at least two pathologists and no patients had received chemotherapy or radiotherapy prior to surgery. All patients signed informed consent. All procedures involving human participants were in accordance with the ethical standards of the Human Research Ethics Committee at The First Affiliated Hospital of Zhengzhou University.

Microarray analysis

The general profiles of human lncRNAs and protein-coding transcripts from the three cases of cervical cancer and adjacent noncancerous tissues were detected using the Arraystar Human lncRNA Microarray V3.0 (Arraystar, Inc., Rockville, MD, USA). Array images were analyzed by Agilent Feature Extraction software (version 11.0.1.1; Agilent Technologies, Inc.). Differentially expressed genes were identified through the random variance model. A *P* value was calculated using the paired t-test. The threshold set for up- and down-regulated genes was a fold change ≥ 3.0 and a *P* value < 0.05 .

5' and 3' Rapid Amplification of cDNA Ends (RACE)

To determine the transcriptional initiation and termination sites of Inc-UICC, 5'-RACE and 3'-RACE analyses were performed by using a SMARTer™ RACE cDNA Amplification Kit (Clontech, Palo Alto, CA) according to the manufacturer's instructions.

Lentiviral vector construction, production and transfection

The shRNAs targeting Inc-UICC sequences were designed. The target sequence for shUICC-1 (KD1) is 5'-CTCCGAACACATCTGAACA-3'; the sequence for shUICC-2 (KD2) is 5'-CACCAATCCGGACACAAT-3'. Scramble shRNA was used as the negative control (NC). Human Inc-UICC full-length cDNA was amplified by PCR from the mRNA of HeLa cells. The objective products were cloned into pLV plasmid. The constructed vectors and the lentivirus packaging vectors were cotransfected into 293T cells. Lentiviruses were produced, harvested, and purified. Cells were transfected with lentivirus by using 8 $\mu\text{g}/\text{mL}$ polybrene (Sigma, USA). Stable expression cells were selected in 1 $\mu\text{g}/\text{mL}$ puromycin.

RNA isolation and quantitative real-time PCR (qRT-PCR)

The total RNA was isolated using the TRIzol reagent (Invitrogen, USA) according to the manufacturer's instructions. After detection of RNA concentration, 1 μg of total RNA was reversely transcribed with random primers, using the ReverTra Ace® qPCR RT kit (Toyobo, Osaka, Japan). qRT-PCR was performed using the SYBR-Green PCR Master Mix kit (Takara, Japan). Primers for Inc-UICC were as follows: forward: 5'-TCTTGCTACTGCTCACTCTTTG-3'; reverse: 5'-GTGTTCCGGAGTTTCTTCCTTCT-3'. Primers for IL-6 were as follows: forward: 5'-GGAGACTTGCCCTGGTGAAA-3'; reverse: 5'-CTGGC-TTGTTCCTCACTACTC-3'. Primers for GAPDH were as follows: forward: 5'-CAAGAGCACAAAGAGGAAGAGAG-3'; reverse: 5'-CTACATGGCAACTGTGAGGAG-3'. Relative expression was calculated using the 2^{- $\Delta\Delta\text{Ct}$} method.

Cell viability and colony formation

For cell viability detection, 3000 cells per well were seeded in a 96-well plate and were incubated at 37°C. At indicated time point, 10 μL of CCK8 solution (Dojindo, Japan) was added to each well. After 1.5 h, the absorbance was measured by using a micro-plate reader (Bio-Tek Instruments, USA) at 450 nm. For colony formation detection, 2000 cells were planted in 6-well plates and cultured for 2 weeks. Cells were then fixed with 4% paraformaldehyde and stained with 0.5% crystal violet. The assay was performed three times for each treatment.

Inc-UICC promotes cervical cancer progression

Flow cytometric analysis of the cell cycle and apoptosis

For cell cycle detection, cells were harvested, fixed in 70% ethanol, and stained with propidium iodide solution (50 mg/mL propidium iodide, 50 mg/mL RNase A, 0.1% Triton-X, 0.1 mmol/L EDTA). For cell apoptosis detection, cells were stained using an Annexin V-FITC Apoptosis Detection Kit (BD Biosciences). The images of cell cycle and apoptosis were obtained and analyzed, using the FACS Calibur (BD Biosciences, USA) and the Flowjo software (Tree Star Corp, USA).

Migration and invasion assays

Transwell chambers (Corsta) were used to perform the migration and invasion assays. For the migration assay, 1×10^5 cells in a serum-free medium were added to the upper chamber, and 500 μ L of full medium were added to the lower chamber. For the invasion assay, the diluted matrigel (BD Biosciences, USA) paved the upper well of the transwell chamber. After 24 h of incubation, the migratory and invasive cells were fixed with 4% paraformaldehyde, and then stained with crystal violet solution.

Western blot

Cells were lysed using a RIPA buffer, including a protease inhibitor cocktail (Beyotime, Beijing, China). The proteins were separated by SDS-PAGE gels and transferred to PVDF membranes (Millipore, USA). After blocking, the membranes were incubated with primary antibodies at 4°C overnight. The HRP-conjugated secondary antibodies were used to incubate the membranes for 1 h at room temperature. The primary antibodies used were the anti-STAT3 (1:1000, Cell Signaling), the anti-p-STAT3 (1:1000, Cell Signaling), and anti-GAPDH antibody (1:4000, Beverly, USA).

Immunofluorescence (IF) staining

Cells were cultured on a coverslip and fixed with 4% paraformaldehyde. 0.2% Triton X-100 solutions in PBS were used to permeabilize cells for 10 min. After blocking by 1% bovine serum albumin (BSA) for 1 hr, cells were incubated with anti-p-STAT3 antibody (1:200, Cell Signaling) overnight at 4°C. The fluorescence-conjugated secondary antibody (goat-anti-rabbit-Alexa 594-conjugated antibodies,

Life Technologies) was used to incubate the treated coverslips for 1 h at room temperature. The treated coverslips were then incubated with 4',6-Diamidino-2'-phenylindole dihydrochloride (DAPI; Life Technologies) for 3 min at room temperature. The images were obtained using a confocal fluorescence microscope (Olympus, USA).

RNA immunoprecipitation (RIP)

To determine the interaction between Inc-UICC and STAT3, RIP assay was conducted by using Magna RIP RNA Binding Protein Immunoprecipitation Kit (Millipore) according to the manufacturer's instructions.

RNA pull-down

RNA pull-down was performed as previously described [8]. *In vitro* biotin-labeled RNAs (Inc-UICC and its antisense RNA) were transcribed with the biotin RNA labeling mix (Roche) and T7 RNA polymerase (Roche) treated with RNase-free DNase I (Promega) and purified with RNeasy Mini Kit (QIAGEN). Biotinylated RNA was incubated with nuclear extracts of breast cancer cells, and pull-down proteins were run on SDS-PAGE gels. Western blot followed.

Statistical analysis

All data were expressed as the mean \pm SD and analyzed by SPSS Statistics 21. Comparison between groups was analyzed by a Student's *t* test or one-way analysis of variance (ANOVA). The survival rates were analyzed by the Kaplan-Meier estimator. The statistical significance was set at $P < 0.05$.

Results

IncRNAs expression profile in cervical cancer

To identify functional lncRNAs involved in cervical cancer pathogenesis, lncRNA-mRNA co-expression microarray detection was conducted. Hierarchical clustering showed the differential expression levels of lncRNAs between cervical cancer tissues and adjacent non-tumor tissues (**Figure 1A**). To validate the results of microarray analysis, we randomly selected five lncRNAs among these differential lncRNAs and then examined their expression by using qRT-PCR) in 63 pairs of cervical cancer tissues and

Inc-UICC promotes cervical cancer progression

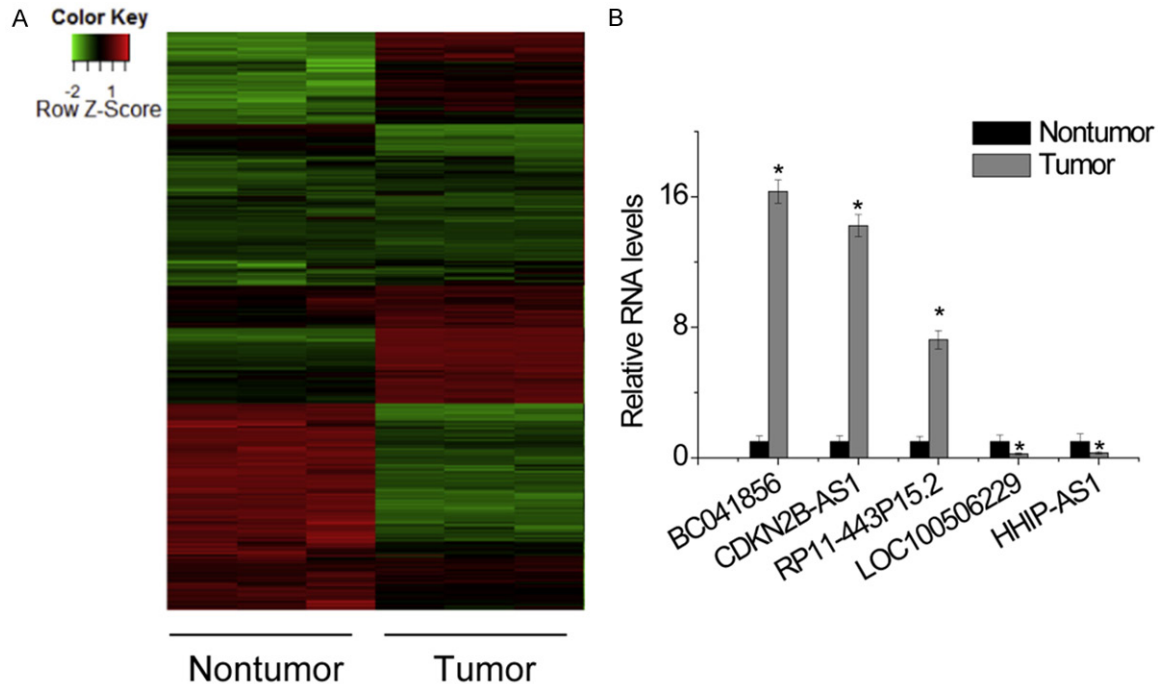


Figure 1. IncRNAs expression profile in cervical cancer. A. Hierarchical clustering reveals distinguishable IncRNA expression profiles between cervical cancer tissues and adjacent non-tumor tissues. B. Five IncRNAs (BC041856, CDKN2B-AS1, and RP11-443P15.2, LOC100506229 and HHIP-AS1) were selected on the basis of the microarray results. The relative expression of indicated IncRNAs in 63 pairs of cervical cancer tissues and adjacent non-tumor tissues was determined by qRT-PCR. * $P < 0.05$.

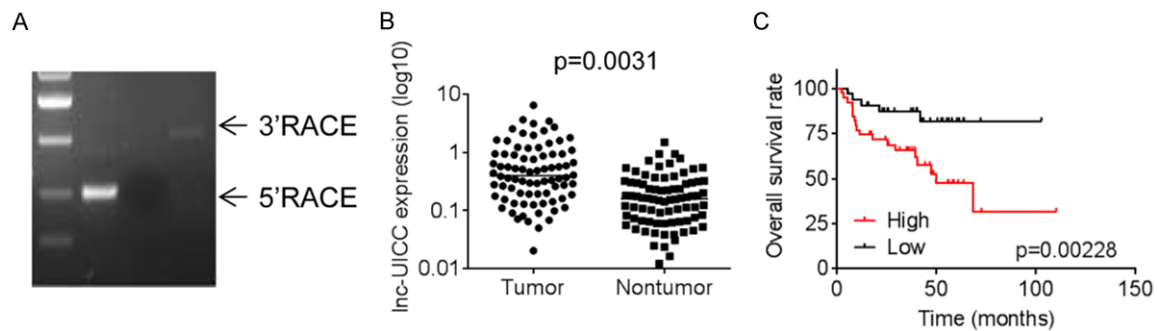


Figure 2. Inc-UICC is overexpressed in cervical cancer and correlates with poor prognosis. A. A representative image of PCR products from the 5'-RACE and 3'-RACE procedure. The major PCR product is marked by an arrow. B. The Inc-UICC expression in 63 pairs of cervical cancer tissues and adjacent non-tumor tissues was examined by qRT-PCR. C. The Kaplan-Meier method was used to determine the survival of 63 patients with cervical cancer and log-rank test to compare survival between the Inc-UICC-high, and Inc-UICC-low groups. The median expression level of Inc-UICC in cervical cancer was used as the cutoff.

adjacent non-tumor tissues. These data confirmed that BC041856, CDKN2B-AS1, and RP11-443P15.2 were overexpressed in cervical cancer, whereas the expression of LOC100506229 and HHIP-AS1 was decreased (**Figure 1B**). Thus, our data indicate that a set of IncRNAs are frequently aberrantly expressed in cervical cancer.

Inc-UICC is overexpressed in cervical cancer and correlates with poor prognosis

We used gene coexpression networks to cluster thousands of transcripts into phenotypically relevant coexpression modules. We focused on coexpression modules that have a high rate of protein-coding RNAs in the cervical cancer

Inc-UICC promotes cervical cancer progression

Table 1. The correlation between Inc-UICC expression and clinical features of cervical cancer patients

Clinical features	Inc-UICC		P value
	High	Low	
Age (years)			
≤40	16	18	0.455
>40	18	14	
Size (cm)			
≥ 4	21	15	0.145
<4	13	19	
FIGO stages			
I-II	9	20	0.007
III-IV	25	14	
Distant metastasis			
Present	23	18	0.215
Absent	11	16	
Lymphatic metastasis			
Present	21	12	0.029
Absent	13	22	

FIGO, International Federation of Gynecology and Obstetrics. The median expression level of Inc-UICC in cervical cancer tissue was used as the cutoff.

coexpression network. Among the differentially expressed lncRNAs, Inc-UICC expression was one of the most significantly overexpressed in the cervical cancer tissues compared to adjacent non-tumor tissues. The role of Inc-UICC in cervical cancer can be characterized by this method. Transcriptional initiation and termination sites of Inc-UICC were then identified by rapid amplification of cDNA ends (RACE) analysis (**Figure 2A**).

Then, we evaluated Inc-UICC expression in 63 paired tissue samples and confirmed the higher levels of Inc-UICC expression in cervical cancer tissue (**Figure 2B**). To investigate the relationship between Inc-UICC expression and cervical cancer clinical features, 68 patients with cervical cancer were divided into high and low Inc-UICC expression level groups based on the median value. As shown in **Table 1**, statistical analysis of clinical characteristics and Inc-UICC expression indicated that overexpression of Inc-UICC was significantly associated with FIGO stage, lymph node metastasis. Moreover, we performed Kaplan-Meier analysis to determine the association between Inc-UICC expression and prognosis of patients with cervical cancer. We found that patients with high Inc-UICC levels had shorter overall survival time (**Figure 1C**). These findings suggest that upreg-

ulation of Inc-UICC is associated with cervical cancer progression and poor prognosis.

Inc-UICC promotes cell growth in vitro and in vivo

After detecting Inc-UICC expression in 5 cervical cancer cell lines (**Figure 3A**), we developed HeLa cells with stably overexpressed Inc-UICC (**Figure 3B**), and SiHa cells with stably silenced Inc-UICC expression (**Figure 3C**). To detect the effect of Inc-UICC on the proliferation of cervical cancer cells, CCK-8 and colony formation assays were performed. The results showed that Inc-UICC overexpression increased the proliferative capacity of HeLa cells, compared to that of control cells (**Figure 3D, 3E**). In contrast, deletion of endogenous Inc-UICC expression significantly decreased the proliferative capacity of SiHa cells (**Figure 3F, 3G**).

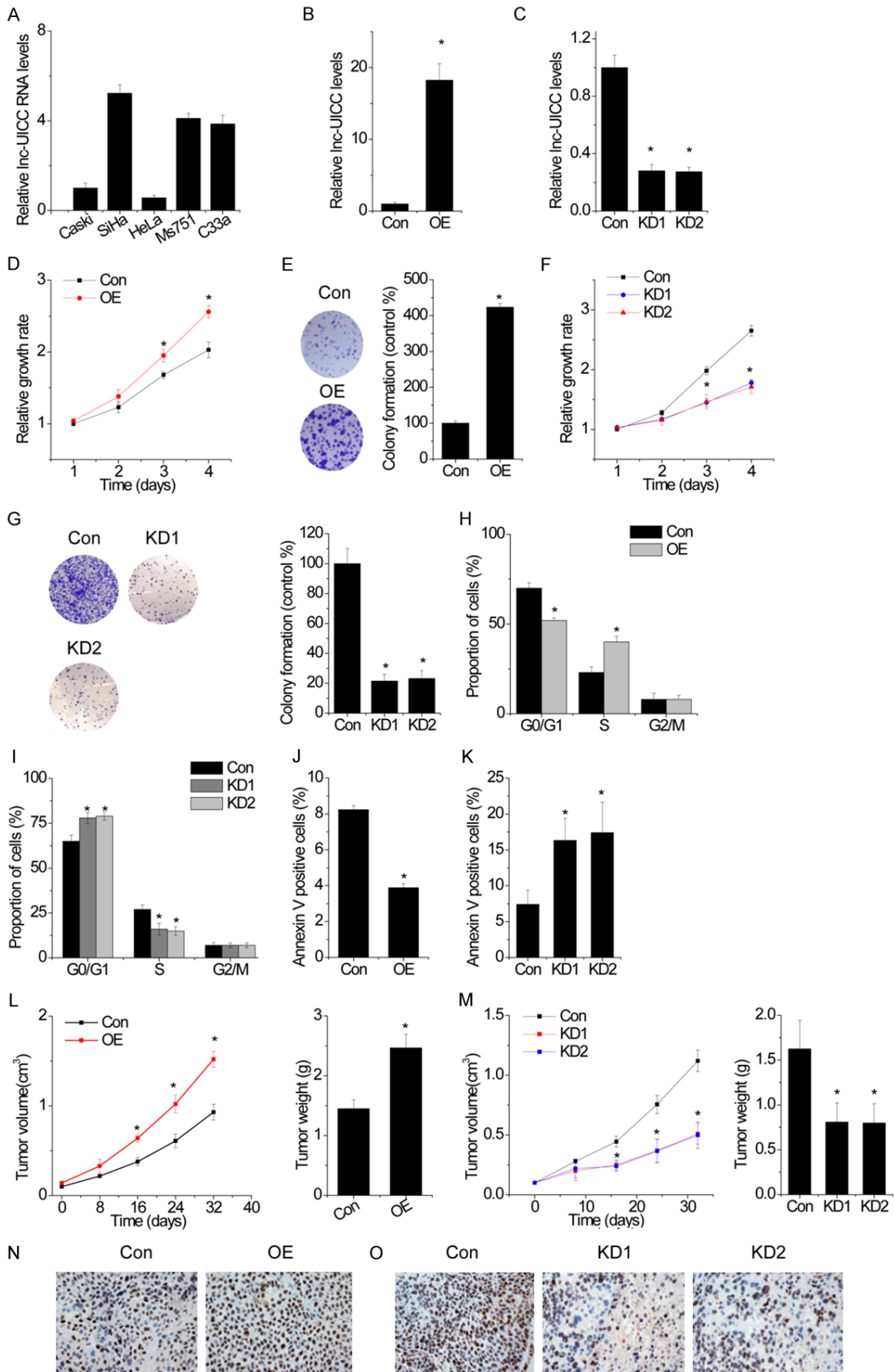
We then analyzed differences in cell cycle distributions and apoptosis following Inc-UICC overexpression or knockdown by flow cytometry. We found that Inc-UICC overexpression drove progression beyond the G1/S transition in HeLa cells, whereas Inc-UICC-knockdown induced G1/S arrest in SiHa cells (**Figure 3H, 3I**). Inc-UICC overexpression inhibited the apoptosis of HeLa cells (**Figure 3J**). In contrast, Inc-UICC-knockdown SiHa cells had a significantly higher percentage of Annexin V-positive cells than control cells (**Figure 3K**).

To validate the role of Inc-UICC in the tumorigenesis of cervical cancer cells, we next injected the above stable cells into nude mice. The result showed that xenograft tumors grown from HeLa cells overexpressing Inc-UICC had larger mean volumes and weights than tumors grown from control cells (**Figure 3L**). Knockdown of Inc-UICC expression dramatically inhibited the tumor growth in both weight and size in nude mice (**Figure 3M**). Moreover, immunohistochemistry analysis indicated that Ki-67 staining was significantly reduced in Inc-UICC knockdown xenograft tumors, while increased in Inc-UICC overexpressed tumors (**Figure 3N, 3O**). Together, our results indicate that Inc-UICC promotes the growth of cervical cancer.

Inc-UICC facilitates cell migration, invasion and metastasis in cervical cancer

To evaluate whether Inc-UICC contributes to the progression of cervical cancer, we determined the effect of Inc-UICC on the migration and

Inc-UICC promotes cervical cancer progression



Inc-UICC promotes cervical cancer progression

Figure 3. Inc-UICC promotes cell growth *in vitro* and *in vivo*. (A) qRT-PCR detected Inc-UICC levels in cervical cancer cells. (B) The validation of stably overexpressing Inc-UICC in HeLa cells via qRT-PCR. Con indicates control group, and OE indicates Inc-UICC overexpression. (C) The validation of stably silencing Inc-UICC in SiHa cells via qRT-PCR. Con indicates control group, and KD indicates Inc-UICC knockdown. (D) Proliferation assay of HeLa cells with Inc-UICC overexpression via CCK-8 detection. (E) Proliferation assay of HeLa cells with Inc-UICC overexpression via colony formation assay. (F) Proliferation assay of SiHa cells with Inc-UICC knockdown via CCK-8 detection. (G) Proliferation assay of SiHa cells with Inc-UICC knockdown via colony formation assay. (H and J) Flow cytometry was performed to assess cell cycle progression (H) and apoptosis (J) of HeLa cells after Inc-UICC overexpression. (I and K) Flow cytometry was performed to assess cell cycle progression (I) and apoptosis (K) of SiHa cells after Inc-UICC knockdown. (L) Inc-UICC overexpression in HeLa cells significantly increases tumor growth in a mouse xenograft model (left). Tumor weights of corresponding mouse xenograft models (right). (M) Inc-UICC knockdown in SiHa cells significantly inhibits tumor growth in a mouse xenograft model (left). Tumor weights of corresponding mouse xenograft models (right). (N and O) Immunohistochemistry (IHC) staining with antibody against proliferation marker Ki-67 in each group. *P<0.05.

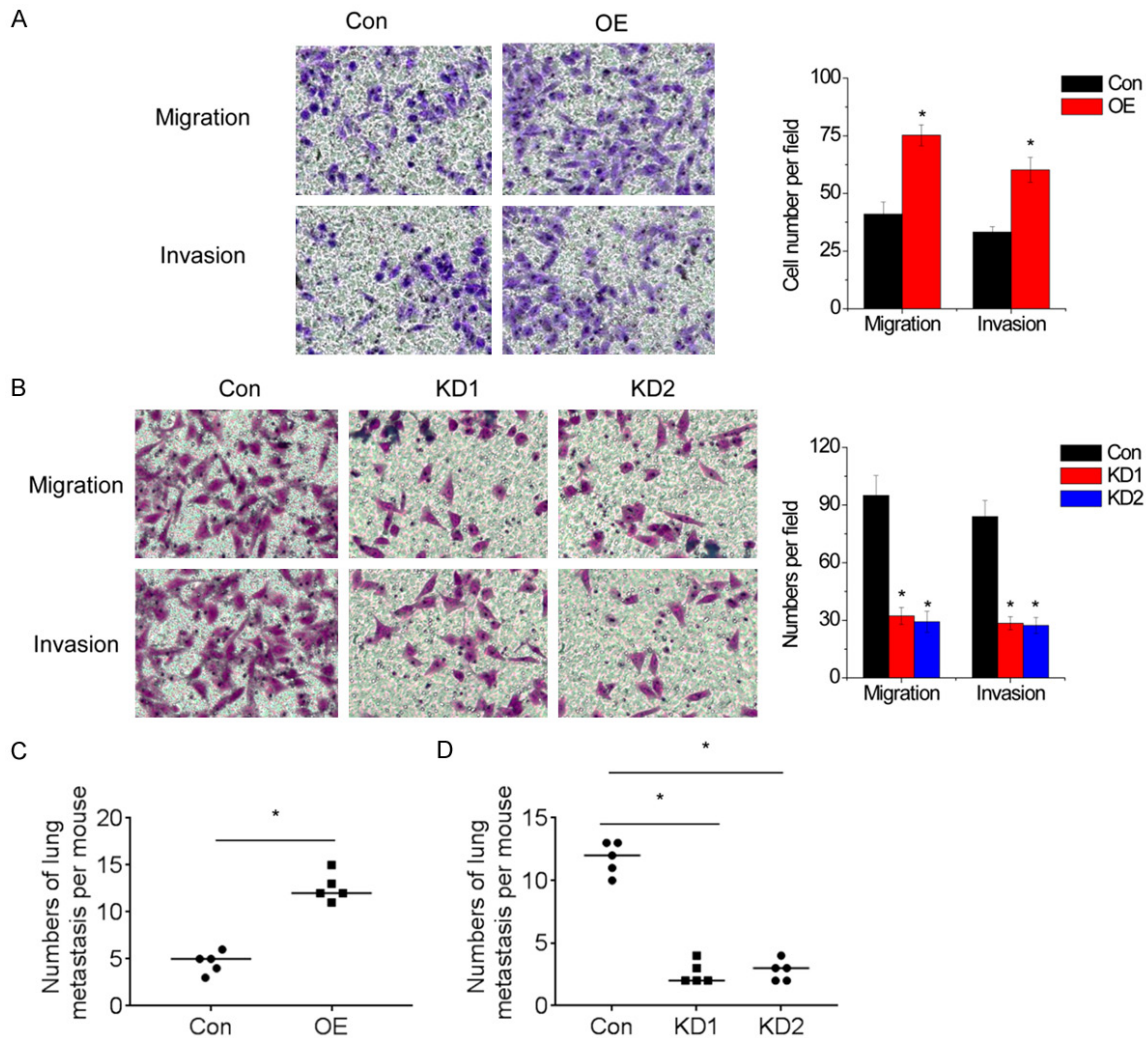


Figure 4. Inc-UICC facilitates cell migration, invasion and metastasis in cervical cancer. A. Transwell migration and invasion assays were performed in HeLa cells with Inc-UICC overexpression. B. Transwell migration and invasion assays were performed in SiHa cells with Inc-UICC knockdown. C. An experimental metastasis animal model was performed by injecting Inc-UICC stable overexpressing HeLa cells into the tail vein of nude mice. The number of tumor nodules on lung surfaces are shown. D. An experimental metastasis animal model was performed by injecting Inc-UICC stable knockdown SiHa cells into the tail vein of nude mice. The number of tumor nodules on lung surfaces are shown. *P<0.05.

Inc-UICC promotes cervical cancer progression

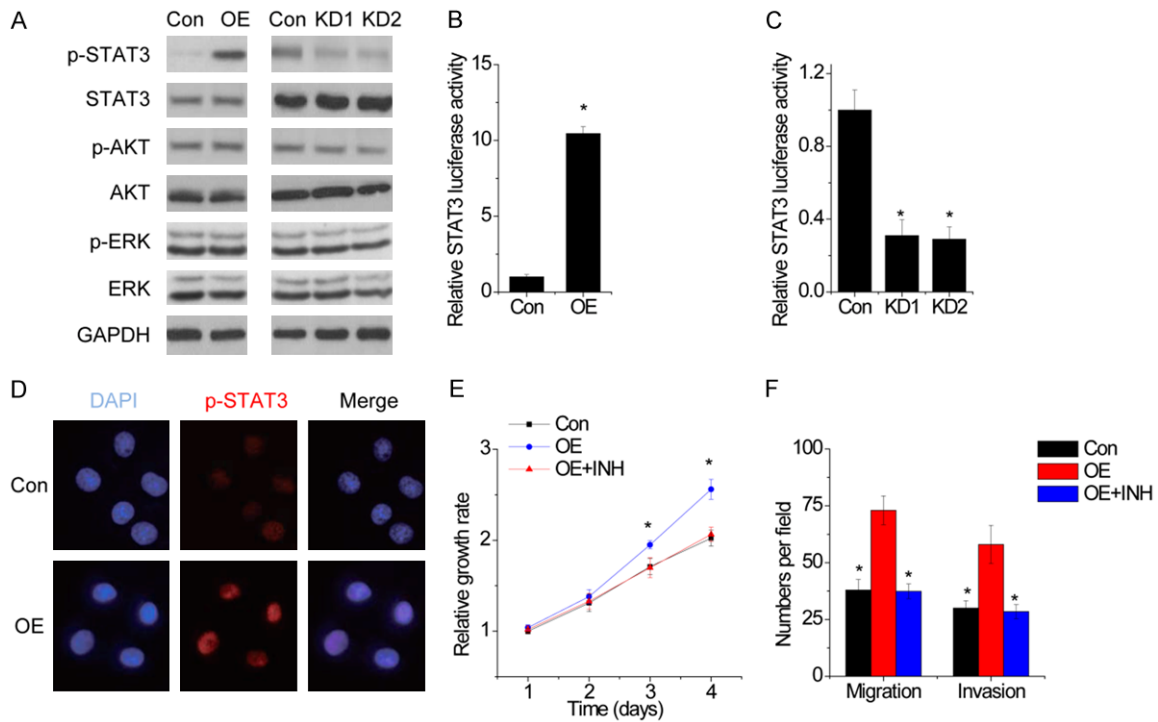


Figure 5. Inc-UICC activates STAT3 signaling. (A) The effect of Inc-UICC overexpression and knockdown on activation of STAT3, AKT and ERK was detected by western blot. (B) Luciferase activity in the lysates of HeLa-Con and HeLa-OE cells transfected with STAT3 response element-luciferase reporter plasmid was measured (normalized by Renilla luciferase activity). (C) Luciferase activity in the lysates of SiHa-Con and SiHa-KD cells transfected with STAT3 response element-luciferase reporter plasmid was measured (normalized by Renilla luciferase activity). (D) p-STAT3 nuclear translocation in HeLa-Con and HeLa-OE cells was analyzed by immunofluorescence assay and representative images were shown. (E and F) The STAT3 inhibitor (INH) S3I-201 (20 μ M) was added to Inc-UICC-overexpressing HeLa cells and the proliferation (E), migration and invasion (F) was detected. * $P < 0.05$.

invasion of HeLa and SiHa cells. Transwell assays showed that overexpression of Inc-UICC dramatically increased cell migration and invasion in HeLa cells (**Figure 4A**). Conversely, Inc-UICC knockdown suppressed the migratory and invasive ability of the cervical cells (**Figure 4B**).

To validate the *in vitro* results, control and Inc-UICC overexpressed HeLa cells were injected into nude mice. As shown in **Figure 4C**, upregulation of Inc-UICC resulted in an increase in metastatic nodules on the mice lungs when compared with those in the control group (**Figure 4C**). On the contrary, knockdown of Inc-UICC suppressed pulmonary metastasis of SiHa cells (**Figure 4D**). These results indicate that Inc-UICC also affects cancer cell migration, invasion and metastasis.

Inc-UICC activates STAT3 signaling

Given the evident effects of Inc-UICC on cervical cancer cell growth and metastasis, signaling pathways involved in tumor growth and

metastasis that might be activated by Inc-UICC were analyzed by examining the expression of phosphorylated forms of STAT3, AKT and ERK using western blot assay (**Figure 5A**). The results indicated that only phospho-STAT3 (p-STAT3) level was observed to be significantly changed by Inc-UICC. Inc-UICC knockdown decreased the phosphorylation of STAT3, whereas Inc-UICC overexpression increased it (**Figure 5A**). STAT3 activation by Inc-UICC was further confirmed by STAT3 reporter assay. STAT3 response element did be activated with Inc-UICC overexpression, but was clearly inhibited with Inc-UICC depletion (**Figure 5B, 5C**). Considering that the p-STAT3 in nucleus is the main executor to activate the transcription of its downstream target genes, we then examined whether the nuclear p-STAT3 accumulation was altered by Inc-UICC. The cellular immunofluorescence assay demonstrated that Inc-UICC induced the nuclear translocation of p-STAT3 protein (**Figure 5D**). Moreover, the treatment of the STAT3 specific inhibitor S3I-

Inc-UICC promotes cervical cancer progression

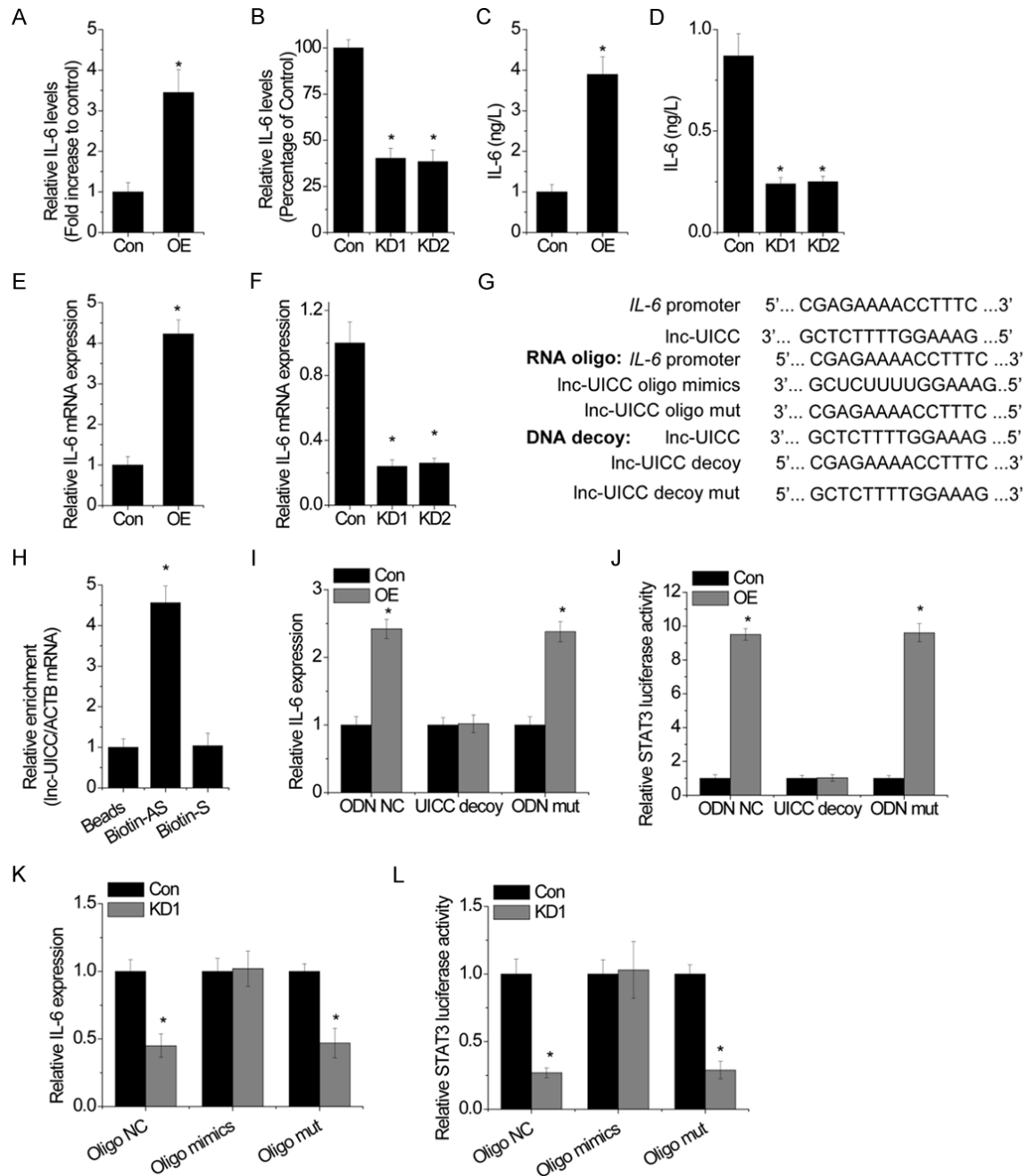


Figure 6. Inc-UICC increases IL-6 transcription. (A and B) mRNA level of IL-6 in Inc-UICC overexpressed (A) or knock-down (B) xenograft. (C and D) Media from the indicated cultured Inc-UICC overexpressed (C) or Inc-UICC knockdown (D) cervical cancer cells was collected and subjected to IL-6 ELISA assays. (E and F) mRNA level of IL-6 in Inc-UICC overexpressed (C) or knockdown (D) cervical cancer cells. (G) The sequence of the predicted Inc-UICC binding locus in *IL-6* promoter is shown. The sequences of oligoribonucleotides (RNA oligo) and oligodeoxynucleotides (DNA decoy) are shown. (H) qRT-PCR analysis of Inc-UICC pulled down by biotin-labeled antisense oligodeoxynucleotide (Biotin-AS) or sense oligodeoxynucleotide (Biotin-S) control in HeLa cells. (I) Transcript of IL-6 was measured in HeLa-Con and HeLa-OE cells transfected with 200 nM oligodeoxynucleotides negative control (ODN NC), Inc-UICC oligodeoxynucleotides decoy (UICC decoy) or mutated oligodeoxynucleotides (ODN mut) was measured by qRT-PCR analysis. (J) STAT3 activity was measured in HeLa-Con and HeLa-OE cells transfected with 200 nM oligodeoxynucleotides negative control (ODN NC), Inc-UICC oligodeoxynucleotides decoy (UICC decoy) or mutated oligodeoxynucleotides (ODN mut) by luciferase activity analysis. (K) Transcript of IL-6 in SiHa-Con and SiHa-KD1 cells transfected with oligoribonucleotide negative control (oligo NC), oligo mimics or oligo mut (200 nM) by qRT-PCR analysis. (L) STAT3 activity in SiHa-Con and SiHa-KD1 cells transfected with oligoribonucleotide negative control (oligo NC), oligo mimics or oligo mut (200 nM) was measured by luciferase activity analysis. *P<0.05.

201 diminished the the capacities of cellular proliferation, migration and invasion between lnc-UICC overexpressing HeLa cells and control cells (**Figure 5E, 5F**), suggesting that lnc-UICC promoted malignant progression of cervical cancer cells by activating STAT3 signaling. These results suggested that STAT3 signaling played a crucial role in mediating lnc-UICC's function.

lnc-UICC increases IL-6 transcription

We next sought to elucidate whether STAT3 activation induced by lnc-UICC was dependent on IL-6. The IL-6 mRNA level of subcutaneous xenograft tumors was dramatically increased in the lnc-UICC overexpressed group (**Figure 6A**) compared with that in the control group. Meanwhile, IL-6 mRNA was significantly decreased in the lnc-UICC knockdown subcutaneous xenograft tumors compared with that in the control group (**Figure 6B**). To validate that lnc-UICC could regulate the IL-6 level, the protein in the cell culture supernatants of the cultured cervical cancer cells with lnc-UICC alteration was examined by ELISA assay. IL-6 protein level was increased in HeLa-OE cells compared with that in the vector control cells (**Figure 6C**), whereas it was significantly decreased in SiHa-KD cells compared with that in control cells (**Figure 6D**). Consistently, IL-6 mRNA level was also affected by lnc-UICC in HeLa and SiHa cells (**Figure 6E, 6F**).

Next, we identified one putative lnc-UICC complementary binding locus within the IL-6 promoter region (671 bp from the transcription start site) using Basic Local Alignment Search Tool (BLAST) (**Figure 6G**). A biotin-labeled anti-sense oligodeoxynucleotide (Biotin-AS), complementary to the sequence of human lnc-UICC at the binding locus in IL-6 promoter, was synthesized for the biotin pull down assay. As shown in **Figure 6H**, lnc-UICC was significantly enriched in the AS-biotin pull down group compared with the sense oligodeoxynucleotide (Biotin-S) control group of SiHa cells. To further confirm the interaction between lnc-UICC and IL-6 promoter, an oligoribonucleotide (oligo mimics) and an oligodeoxynucleotide (ODN) decoy as well as their corresponding mutated controls (Oligo mut/ODN mut) were designed according to the sequence of the binding locus (**Figure 6G**). As shown in **Figure 6I, 6J**, the increase of IL-6 transcription and STAT3 activa-

tion of lnc-UICC-OE cells was abolished by the ODN decoy but not ODN mut. Consistently, the oligo mimics abrogated the suppression of IL-6 transcription and STAT3 inactivation of lnc-UICC-KD cells compared with control cells, but the mutated control exhibited no influence (**Figure 6K, 6L**).

lnc-UICC interacts with STAT3 protein

To further seek out the underlying mechanism of lnc-UICC inducing STAT3 activation, we performed RNA pull-down and mass spectrometry (MS) analysis. Intriguingly, we found p-STAT3 was a potential lnc-UICC-interacting candidate. To verify the interaction between lnc-UICC and p-STAT3, RNA immunoprecipitation (RIP) assay was used. The result showed that lnc-UICC transcript was robustly enriched by p-STAT3 antibody (**Figure 7A**). RNA pull-down assay was further used to validate the interaction between lnc-UICC and p-STAT3 (**Figure 7B**).

Furthermore, to determine the mechanism by which lnc-UICC regulated p-STAT3, we detected the effect of lnc-UICC on pSTAT3 protein stability. After treatment of protein synthesis inhibitor cycloheximide (CHX), p-STAT3 protein half-life was markedly prolonged by lnc-UICC overexpression (**Figure 7C**), while the stability of p-STAT3 was markedly suppressed by lnc-UICC knockdown (**Figure 7D**). Moreover, lnc-UICC overexpression dramatically suppressed ubiquitination level of p-STAT3 protein, whereas depletion of lnc-UICC exerted opposite function (**Figure 7E**). Subsequently, we found the upregulation of p-STAT3 protein levels induced by lnc-UICC overexpression were abolished after proteasomal degradation was blocked by MG-132 (**Figure 7F**). These results demonstrate that lnc-UICC can associate with p-STAT3 to increase its protein stability.

IL-6/STAT3 signaling activates lnc-UICC transcription to form a positive feed-back regulatory loop

As IL-6/STAT3 signaling shares a longstanding association with cervical cancer carcinogenesis, we investigated whether IL-6 could regulate lnc-UICC. Recombinant human IL-6 (rhIL-6) treatment increased the lnc-UICC expression both in HeLa and SiHa cells (**Figure 8A**). Moreover, we transfected IL-6 siRNA into cervical cancer cells and found that IL-6-siRNA significantly decreased lnc-UICC expression (Fi-

Inc-UICC promotes cervical cancer progression

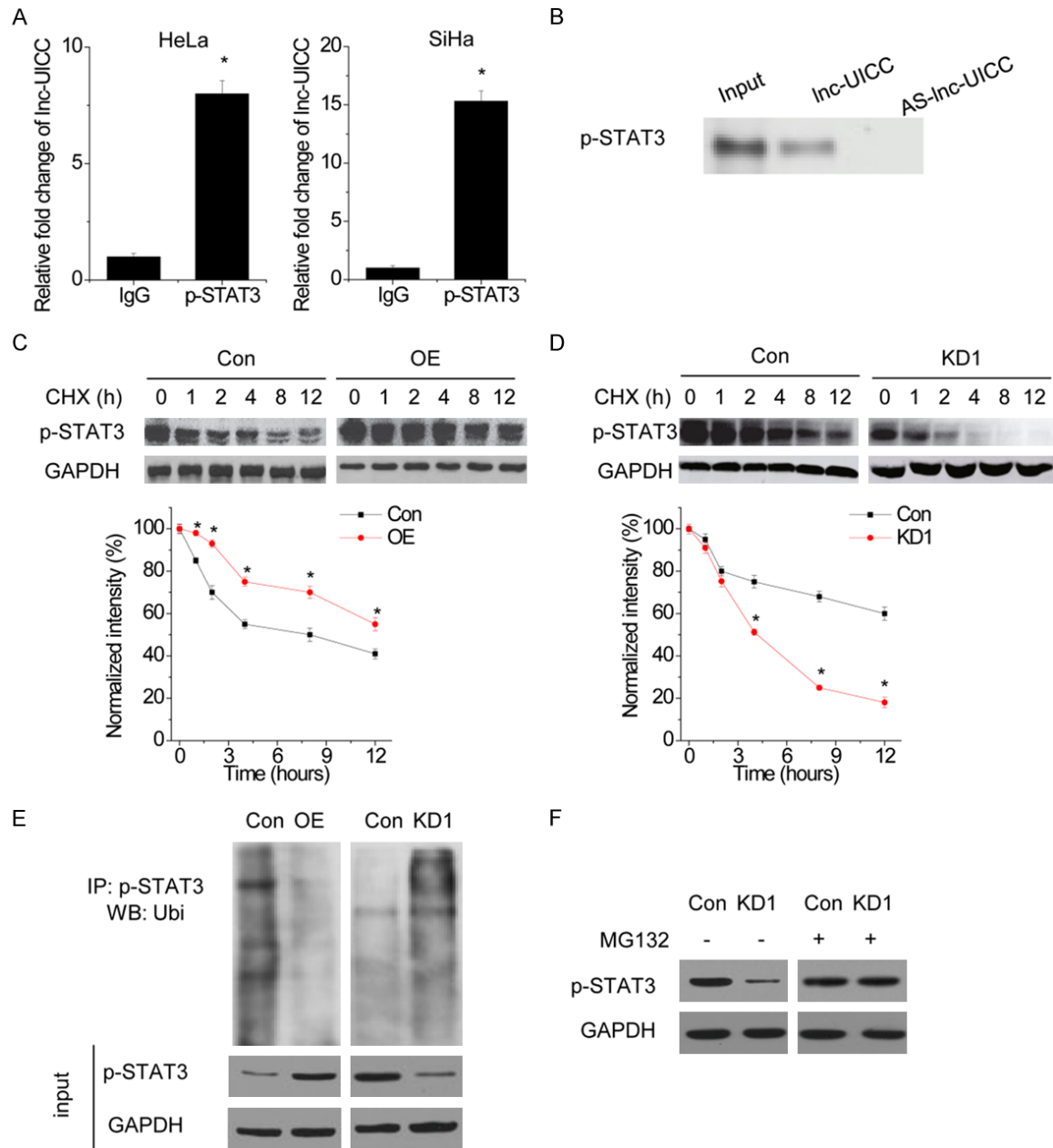


Figure 7. Inc-UICC interacts with p-STAT3 protein. A. The RIP assay was performed to determine the interaction between Inc-UICC and p-STAT3. The IgG was taken as negative control. B. The RNA pull down assay was performed to determine the interaction between Inc-UICC and p-STAT3. Antisense (AS) Inc-UICC was taken as negative control. C. HeLa cells with or without Inc-UICC overexpression were treated with CHX (100 mg/ml) for the indicated time points. The cell lysates were examined by immunoblotting (up panel). A plot of normalized amount of p-STAT3 protein is shown (down panel). D. HeLa cells with or without Inc-UICC knockdown were treated with CHX (100 mg/ml) for the indicated time points. The cell lysates were examined by immunoblotting (up panel). A plot of normalized amount of p-STAT3 protein is shown (down panel). E. Western blot of p-STAT3-associated ubiquitination in cervical cancer cells with Inc-UICC overexpression (left panel) or knockdown (right panel). F. Western blot of p-STAT3 expression in SiHa-Con and SiHa-KD1 cells treated with vehicle control or MG132. *P<0.05.

Figure 8B), suggesting IL-6 could indeed regulate Inc-UICC expression.

Of note, we discovered three putative STAT3-binding elements within Inc-UICC promoter

region through JASPAR bioinformatics analysis (Figure 8C). We further investigated whether IL-6/STAT3 could regulate Inc-UICC expression in turn. STAT3 inhibitor or siRNA significantly decreased Inc-UICC transcription in HeLa cells

Inc-UICC promotes cervical cancer progression

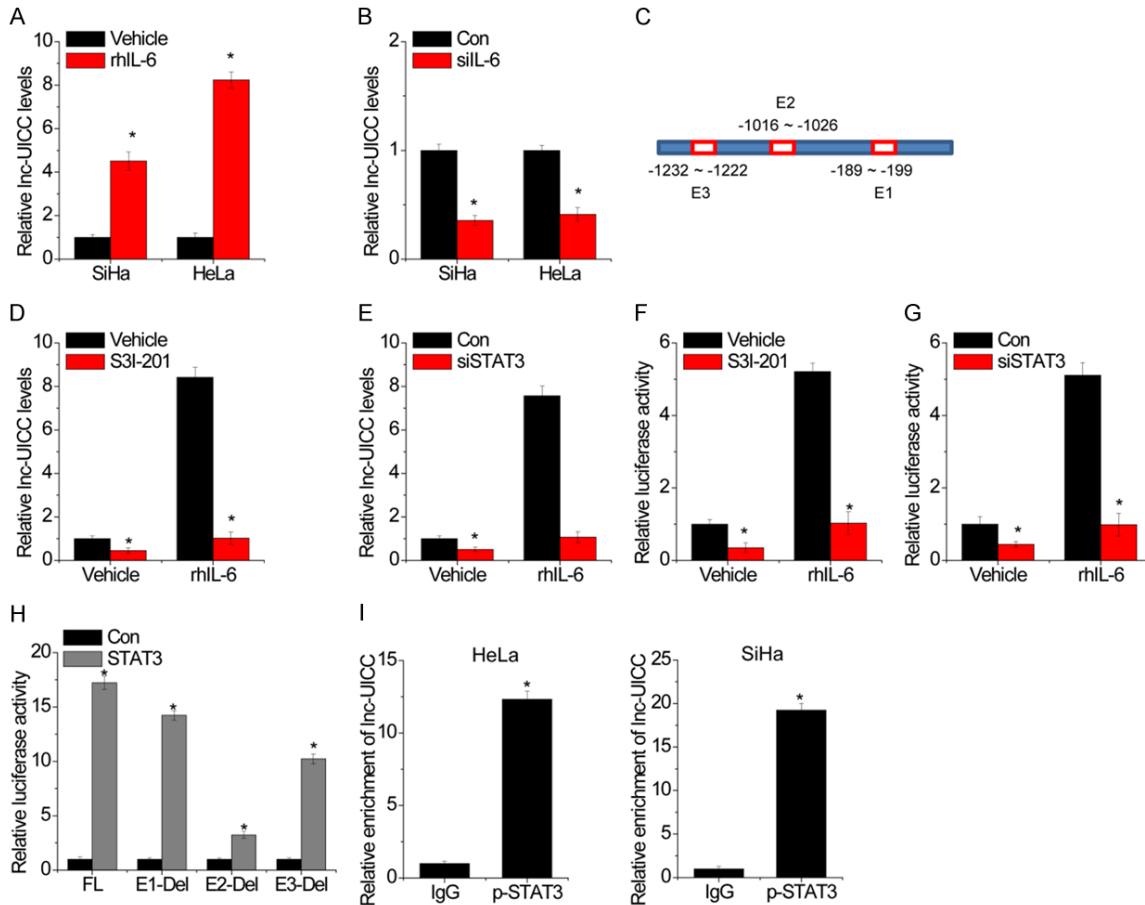


Figure 8. IL-6/STAT3 activates Inc-UICC transcription to form a positive feed-back regulatory loop. A. The cervical cancer cells were treated with 10 ng/mL rhIL-6 for 12 hours. The Inc-UICC was then detected by qRT-PCR. B. The cervical cancer cells were transfected with IL-6 siRNA. After 48h, the Inc-UICC was then detected by qRT-PCR. C. Schematic diagram of canonical STAT3-binding motif (JASPAR Database) and three potential STAT3 responsive elements (E1, E2, and E3) in the Inc-UICC promoter region. D. Inc-UICC RNA levels when 20 μ M STAT3 inhibitor and 10 ng/mL rhIL-6 was used to treat cells. E. Inc-UICC RNA levels when STAT3 siRNA and 10 ng/mL rhIL-6 was used to treat cells. F. Inc-UICC promoter luciferase activity when 20 μ M STAT3 inhibitor and 10 ng/mL rhIL-6 was used to treat cells. G. Inc-UICC promoter luciferase activity and 10 ng/mL rhIL-6 was used to treat cells. H. Three predicted STAT3-binding sites of the Inc-UICC promoter was individually deleted and named E1-Del, E2-Del, and E3-Del. Luciferase assay was employed to detect transcriptional activities of the three Inc-UICC promoter deletion mutants when STAT3 expression was enforced in HeLa cells. FL indicates Full-length Inc-UICC promoter sequence. I. ChIP assays showed that STAT3 bound to the E2 element of Inc-UICC promoter. IgG served as a negative control. *P<0.05.

treated with or without rhIL-6 (Figure 8D, 8E). Luciferase assay indicated the Inc-UICC promoter was repressed by STAT3 inhibitor or siRNA (Figure 8F, 8G). To clarify which element was necessary for STAT3-mediated Inc-UICC expression, the three predicted STAT3-binding sites were individually deleted. We found STAT3 nearly failed to promote Inc-UICC transcriptional activity without the E2 element, while E1 and E3 absence only downregulated Inc-UICC promoter activity in part (Figure 8H), indicating that the E2 element was essential for STAT3 to activate Inc-UICC transcription. To further confirm this result, ChIP assay was performed

with p-STAT3 antibody, followed by qRT-PCR detection with specific primer for E2 element. As shown in Figure 8I, STAT3 could associate with Inc-UICC promoter and were enriched within the E2 region. These findings suggest that there is a regulatory feed-back loop between Inc-UICC and IL-6/STAT3 signaling, which may continuously activate their oncogenic functions.

Discussion

Emerging evidence has indicated the regulatory role of lncRNAs in various cancers including

lnc-UICC promotes cervical cancer progression

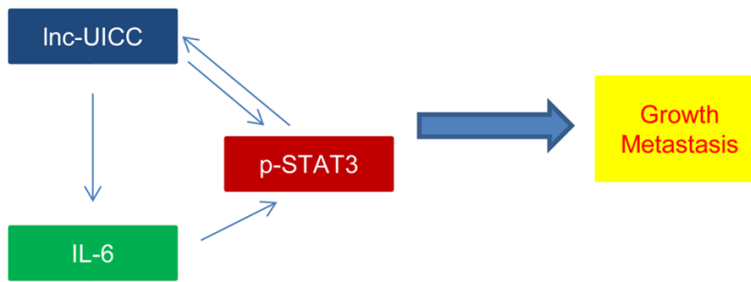


Figure 9. Schematic diagram of lnc-UICC regulating progression via activating the IL-6/STAT3 signaling in cervical cancer.

cervical cancer. However, the mechanism of specific lncRNA remains largely unclear. Here, we report that lncUICC acts as an oncogene in cervical cancer progression. As described in **Figure 9**, lnc-UICC bound to IL-6 promoter to activate its transcription. lnc-UICC also binds to p-STAT3 protein and protects it from degradation. As a result, STAT3 signaling pathway is activated by lnc-UICC, thereby inducing growth and metastasis. Meanwhile, the activated STAT3 reciprocally triggers lnc-UICC transcription to sustain the oncogenic effect of the lnc-UICC/IL-6/STAT3 axis continuously.

Increasing evidence has demonstrated that lncRNAs regulate biological behavior of malignant tumors. For instance, increase of lncRNA HOTAIR in cervical cancer cells upregulated VEGF, MMP-9 and genes associated with epithelial mesenchymal transition for enhancement of tumor invasion [9]. Overexpression of lncRNA MALAT-1 in cancer tissues was linked to tumor cell differentiation, lymph node metastasis and prognosis [10]. Moreover, lncRNA LET downregulation was associated with prognosis of cervical cancer and inhibited the progression of bladder cancer and gastric cancer [11-13]. This study, for the first time, reported that lnc-UICC expression significantly increased in cervical cancer tissue. lnc-UICC expression was correlated with FIGO stage, lymph node metastasis. The Kaplan-Meier analysis illustrated that high levels of lnc-UICC correlated with worse overall survival of cervical cancer patients, revealing that lnc-UICC might be an important regulator in the pathogenesis of cervical cancer.

STAT3 plays central roles in cancer development, which can regulate a number of genes expression to promote cell proliferation, metastasis, immunosuppression, and angiogenesis [14]. Currently, several lncRNAs have been doc-

umented to affect the activation of STAT3. For example, lncRNA-DILC and lncRNA-SRLR can indirectly modulate STAT3 signaling through regulating IL-6 expression [15, 16], and IL-6 is the most well-established upstream activator of STAT3. Our *in vitro* and *in vivo* assays demonstrated that IL-6/STAT3 signaling was responsible for lnc-UICC mediated growth and metastasis

of cervical cancer. lnc-UICC could increase the phosphorylation of STAT3. We further showed that the lnc-UICC promoted STAT3 activation through two different ways. lnc-UICC could regulate the IL-6 transcription through binding to IL-6 promoter. A recent study demonstrated that nuclear localized lncRNAs can participate in the regulation transcription processes through binding to active chromatin sites [17]. Intriguingly, we identified a putative binding locus of lnc-UICC within the IL-6 promoter region through bioinformatics prediction, which was further confirmed by pull down assay. The alteration of IL-6 expression and STAT3 activation induced by lnc-UICC overexpression and lnc-UICC knockdown were abolished by the ODN decoy and oligo mimics of lnc-UICC, respectively, which further indicates the interaction of lnc-UICC with IL-6 promoter. On the other hand, lnc-UICC also has the capacity to regulate STAT3. We found the binding of lnc-UICC can protect p-STAT3 protein from proteasomal degradation, which increases its stability and induces the activation of STAT3. In future, it would be of interest to identify their binding fragments, and determine the underlying mechanism of p-STAT3 stability mediated by lnc-UICC.

In conclusion, our study showed that lnc-UICC was overexpressed in cervical cancer tissue, and upregulation of lnc-UICC could promote growth and metastasis of cervical cancer. Our study elucidated a novel pathway in lnc-UICC-mediated growth and metastasis, which suggested new therapeutic targets, including lnc-UICC/IL-6/STAT3 signaling pathway, in the prevention and treatment of cervical cancer. Further work should be performed to obtain more information about lnc-UICC, and to explore the clinical diagnosis value and develop new drug therapy for cervical cancer.

Disclosure of conflict of interest

None.

Address correspondence to: Dr. Qian Zhao, Department of Gynecology, The First Affiliated Hospital of Zhengzhou University, Zhengzhou 450052, Henan Province, P. R. China. E-mail: zhaoqianzzu@yeah.net

References

- [1] Jemal A, Bray F, Center MM, Ferlay J, Ward E and Forman D. Global cancer statistics. *CA Cancer J Clin* 2011; 61: 69-90.
- [2] Hockel M, Hentschel B and Horn LC. Association between developmental steps in the organogenesis of the uterine cervix and locoregional progression of cervical cancer: a prospective clinicopathological analysis. *Lancet Oncol* 2014; 15: 445-456.
- [3] Zhu P, Wang Y, Wu J, Huang G, Liu B, Ye B, Du Y, Gao G, Tian Y, He L and Fan Z. LncBRM initiates YAP1 signalling activation to drive self-renewal of liver cancer stem cells. *Nat Commun* 2016; 7: 13608.
- [4] Hu G, Niu F, Humburg BA, Liao K, Bendi S, Calten S, Fox HS and Buch S. Molecular mechanisms of long noncoding RNAs and their role in disease pathogenesis. *Oncotarget* 2018; 9: 18648-18663.
- [5] Peng Z, Liu C and Wu M. New insights into long noncoding RNAs and their roles in glioma. *Mol Cancer* 2018; 17: 61.
- [6] Morlando M and Fatica A. Alteration of epigenetic regulation by long noncoding RNAs in cancer. *Int J Mol Sci* 2018; 19.
- [7] Peng L, Yuan X, Jiang B, Tang Z and Li GC. LncRNAs: key players and novel insights into cervical cancer. *Tumour Biol* 2016; 37: 2779-2788.
- [8] Hu X, Feng Y, Zhang D, Zhao SD, Hu Z, Greshock J, Zhang Y, Yang L, Zhong X, Wang LP, Jean S, Li C, Huang Q, Katsaros D, Montone KT, Tanyi JL, Lu Y, Boyd J, Nathanson KL, Li H, Mills GB and Zhang L. A functional genomic approach identifies FAL1 as an oncogenic long noncoding RNA that associates with BMI1 and represses p21 expression in cancer. *Cancer Cell* 2014; 26: 344-357.
- [9] Yang T, He X, Chen A, Tan K and Du X. LncRNA HOTAIR contributes to the malignancy of hepatocellular carcinoma by enhancing epithelial-mesenchymal transition via sponging miR-23b-3p from ZEB1. *Gene* 2018; 670: 114-122.
- [10] Zhang Y, Wang T, Huang HQ, Li W, Cheng XL and Yang J. Human MALAT-1 long non-coding RNA is overexpressed in cervical cancer metastasis and promotes cell proliferation, invasion and migration. *J BUON* 2015; 20: 1497-1503.
- [11] Mao Z, Li H, Du B, Cui K, Xing Y, Zhao X and Zai S. LncRNA DANCR promotes migration and invasion through suppression of lncRNA-LET in gastric cancer cells. *Biosci Rep* 2017; 37.
- [12] Jiang S, Wang HL and Yang J. Low expression of long non-coding RNA LET inhibits carcinogenesis of cervical cancer. *Int J Clin Exp Pathol* 2015; 8: 806-811.
- [13] Ma MZ, Kong X, Weng MZ, Zhang MD, Qin YY, Gong W, Zhang WJ and Quan ZW. Long non-coding RNA-LET is a positive prognostic factor and exhibits tumor-suppressive activity in gallbladder cancer. *Mol Carcinog* 2015; 54: 1397-1406.
- [14] Johnson DE, O'Keefe RA and Grandis JR. Targeting the IL-6/JAK/STAT3 signalling axis in cancer. *Nat Rev Clin Oncol* 2018; 15: 234-248.
- [15] Wang X, Sun W, Shen W, Xia M, Chen C, Xiang D, Ning B, Cui X, Li H, Li X, Ding J and Wang H. Long non-coding RNA DILC regulates liver cancer stem cells via IL-6/STAT3 axis. *J Hepatol* 2016; 64: 1283-1294.
- [16] Xu Z, Yang F, Wei D, Liu B, Chen C, Bao Y, Wu Z, Wu D, Tan H, Li J, Wang J, Liu J, Sun S, Qu L and Wang L. Long noncoding RNA-SRLR elicits intrinsic sorafenib resistance via evoking IL-6/STAT3 axis in renal cell carcinoma. *Oncogene* 2017; 36: 1965-1977.
- [17] West JA, Davis CP, Sunwoo H, Simon MD, Sadreyev RI, Wang PI, Tolstorukov MY and Kingston RE. The long noncoding RNAs NEAT1 and MALAT1 bind active chromatin sites. *Mol Cell* 2014; 55: 791-802.